DOI: 10.1002/ejoc.201000792

Photooxidation of Dithiaethyneporphyrin

Anna Berlicka,[a] Lechosław Latos-Grażyński,*[a] Ludmiła Szterenberg,[a] and Miłosz Pawlicki[a]

Keywords: Porphyrinoids / Photooxidation / Degradation / Isomerization / Cleavage reactions

The oxidative degradation of the contracted carbaporphyrinoid 3,8,13,18-tetraphenyldithiaethyneporphyrin, which contains an acetylene moiety embedded in the macrocyclic framework, was investigated. The light-induced, regioselective cleavage of the macrocyclic ring was observed during exposure to dioxygen affording four open-chain diastereomers terminated by carbonyl groups. Studies on the regioselectivity of the process showed that the thiophene was cleft together with the 8-aryl substituent, which proved the primary attack of dioxygen at the C8–C9 bond. Diastereomers {4*Z*,10*E*}, {4*Z*,10*Z*}, {4*E*,10*E*}, and {4*E*,10*Z*} [the arrangement with respect to C4–C5 and C10···C13 conjugated bonds given] differ by the orientation of the terminal pyrrolone unit with respect to the 5-phenyl substituent and by the geometry around the cumulene fragment. Thermal {4*Z*,10*E*}–{4*Z*,10*Z*} and {4*E*,10*E*}–{4*E*,10*Z*} isomerization was detected and was confirmed by exchange cross-peaks in the ROESY map. The molecular structures of the {4*Z*,10*E*} and {4*E*,10*E*} stereoisomers were established by X-ray analysis. Density functional theory (DFT) was applied to model the molecular and electronic structure of {4*Z*,10*E*}, {4*Z*,10*Z*}, {4*E*,10*E*}, and {4*E*,10*Z*}. The very small energy difference observed between suitable diastereomers accounts for their coexistence in solution (0.48 kcal/mol for {4*Z*,10*E*}, {4*Z*,10*Z*}; 0.63 kcal/mol for {4*E*,10*E*}, {4*E*,10*Z*}).

Introduction

Ethyneporphyrins, representing a novel type of contracted porphyrinoid related to hypothetical [18]triphyrin(4.1.1) where an acetylene unit is embedded in the macrocyclic framework, have been synthesized recently.[1] Aromatic dithiaethyneporphyrin **1** introduces a unique, constitutional pattern created by fusing the constructive motifs of 21,23-dithiaporphyrin and acetylene, whereas weakly aromatic dithiaethyneazuliporphyrin **2**, the first contracted carbaporphyrinoid,[2] combines three different structural elements, acetylene, azulene, and thiophene, in the porphyrin frames (Scheme 1).[1] Very recently it was demonstrated that dithiaethyneporphyrin **1** allows the formation of iron(II) double-decker complex – an atypical coordination mode for contracted porphyrinoids.[3] This result shows a potential that stays in the contracted macrocycles where donors set is accompanied by a proper core size.

Originally, the research focused on porphyrinoids was simply reduced to regular, tetrapyrrolic macrocycles. Nevertheless, the group of contracted macrocycles (i.e., corroles[4]), but especially in a triheterocyclic variant, has gained much attention in the last few years. The rise in interest was caused by reports on the synthesis of subporphyrins, the new, genuine contracted, aromatic 14π-electron porphyrins,[5,6] simply related to subphthalocyanines, the macrocycles widely explored because of their specific optical properties.[7]

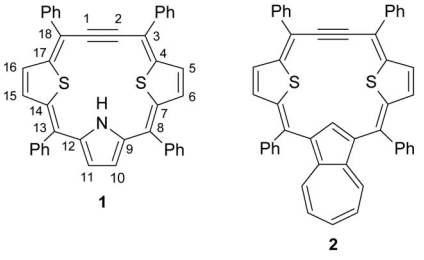

Scheme 1. Structure of dithiaethyneporphyrin **1** and dithiaethyneazuliporphyrin **2**.

The initial, synthetic reports on subporphyrins triggered a variety of peripheral modifications of their skeleton displaying a significant influence of *meso*- and β-substituents on electrochemical and optical properties.[8] Interestingly, the new types of contracted porphyrinoids, imprinted into the *N*-fused porphyrin frame, have been obtained recently by insertion of boron(III),[9] silicon(IV),[10] or phosphorus(V)[11] into *N*-confused porphyrin or phosphorus(V) into 21-telluraporphyrin.[12]

The oxidative cleavage of porphyrinoids is an important reaction in the context of natural processes such as heme catabolism and chlorophyll degradation.[13,14] Chemical oxidation involving a variety of reagents [e.g., H_2O_2 in pyridine,[15] cerium(IV) and thallium(III) salts[16]] and a cou-

[a] Department of Chemistry, University of Wrocław,
14 F. Joliot-Curie St., 50383 Wrocław, Poland
Fax: +48-71-328-2348
E-mail: llg@wchuwr.pl

Supporting information for this article is available on the WWW under http://dx.doi.org/10.1002/ejoc.201000792.

pled oxidation of porphyrin complexes of redox active metals have been involved in the model investigations of heme degradation.[17] Porphyrin ring-opening reactions followed by photooxidation afforded oligopyrrole linear compounds.[18] Formylbiliverdins (**3**) and biliverdins (formed by extrusion of CO) are typically produced in degradation of *meso* unsubstituted porphyrins.[19] The photooxidation of *meso*-tetraarylporphyrins complexes yielded aroyl-substituted bilinone (**4**; Scheme 2).[20]

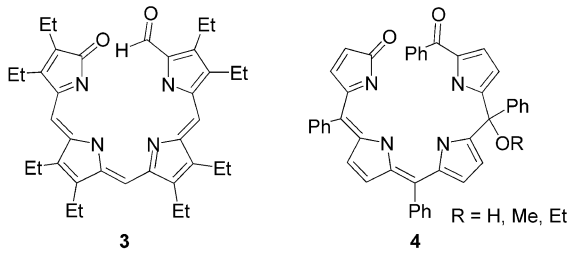

Scheme 2. Structures of the ring-opening products of octaethylporphyrin **3** and tetraphenylporphyrin **4**.

The degradation of *X*-confused porphyrins has been limitedly studied. Initially, Furuta et al. found that during copper(II) insertion to *N*-confused porphyrin in the presence of air linear tripyrrole **5** was formed (Scheme 3).[21] In this case, dioxygen selectively reacted at the C_α–C_{meso} bond adjacent to the *N*-confused pyrrole. A similar product was observed by Pawlicki et al. in the course of oxygenolysis of the copper(II) complex of pyrrole-appended *O*-confused tetraaryloxaporphyrin. This process was not selective and resulted in the formation of two products caused by direct attack of dioxygen on one of the two C_α–C_{meso} bonds, adjacent to the *O*-confused furan.[22] Recently, *N*-confused biliverdin analogue **6** was obtained by Wojaczyński et al. in the course of photooxidation of the *N*-confused tetraphenylporphyrin dianion (Scheme 3).[23] This is an unprecedented example of a linear tetrapyrrolic compound, which can act as a binucleating ligand with two different coordination environments.

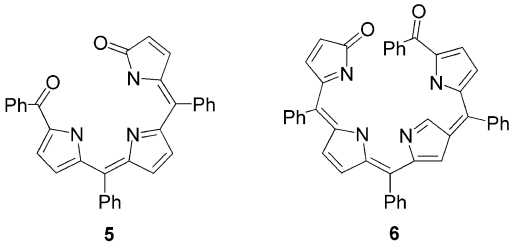

Scheme 3. Degradation products of *N*-confused tetraphenylporphyrin.

To date, the oxidative degradation of contracted porphyrinoids has been investigated in limited quantity. Direct pyrrole–pyrrole bond cleavage by molecular oxygen was observed in the case of 10-phenyl-β-alkylcorroles.[24] Lately, the product of *meso*-triarylcorrole degradation has been identified as a byproduct during the formation of 6-azahemiporphycene.[25] In that case, the ring opening occurs selectively at the 5-*meso* position.

In light of the above, a very sketchy overview, the exploration of porphyrinoid applications raises the problem of their reactivity toward dioxygen and such a question stays in front of the current challenges. Here we report on the photodegradation of dithiaethyneporphyrin. We have found that this contracted porphyrinoid undergoes regioselective cleavage to form four, open-chain diastereomers that have been originally identified through the use of NMR spectroscopic studies.

Results and Discussion

3,8,13,18-Tetraphenyldithiaethyneporphyrin **1** dissolved in dichloromethane during exposure to light undergoes a reaction with air over a period of 20–30 h leading to the regioselective opening of the macrocyclic ring (Scheme 4). The mechanism, including cleavage of the C_α–C_{meso} bonds

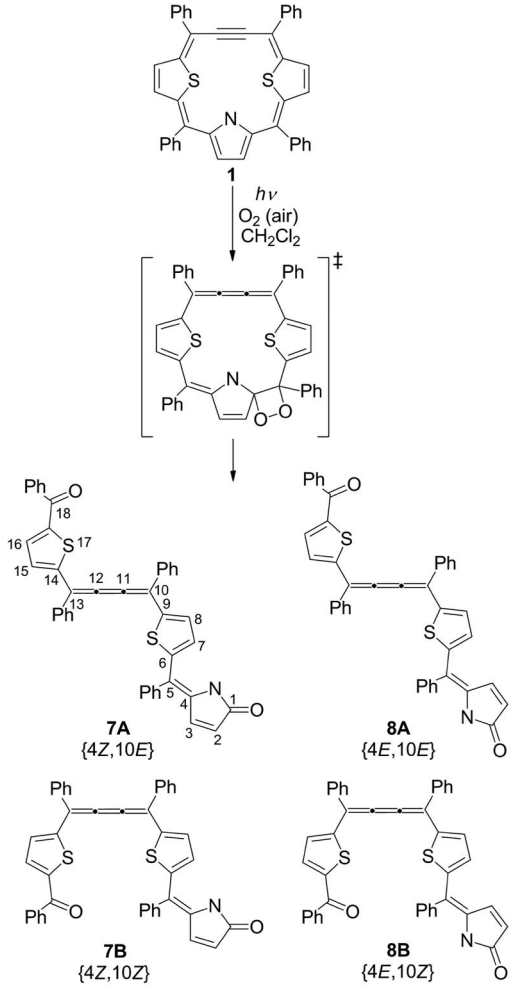

Scheme 4. Photooxidation of dithiaethyneporphyrin **1**. Diastereomers of **7** and **8** as observed by ^{1}H NMR spectroscopy are shown. *E* and *Z* denote the arrangements of the substituents around the C4–C5 bond and the C10–C11–C12–C13 cumulene fragment, respectively.

adjacent to pyrrole by a molecule of dioxygen can be easily applied in this case by analogy to the previously observed reactivity of metal complexes of tetraphenylporphyrin.[20b] Photooxidation introduces a benzoyl group at the α thiophene position and oxygen atom on the terminal *α*-pyrrolic site to afford **7** and **8**. The control experiment proved that both light and dioxygen are necessary to observe the reactivity. A color change from deep orange to pink accompanies the oxidation reaction. Two fractions were easily separated by column chromatography on basic alumina in 70–80 and 10–20% yield, giving stereoisomers **7** and **8**, respectively.

The electronic spectrum of **7** presented in Figure 1 is characterized by broad absorption bands with small extinction coefficients in comparison to parent macrocycle **1**.[1a] For isomers **7A** and **7B**, similar spectra were calculated (Supporting Information, Figure S3 and S4). The UV/Vis spectrum of **7** is consistent with the loss of macrocyclic aromaticity due to ring opening.

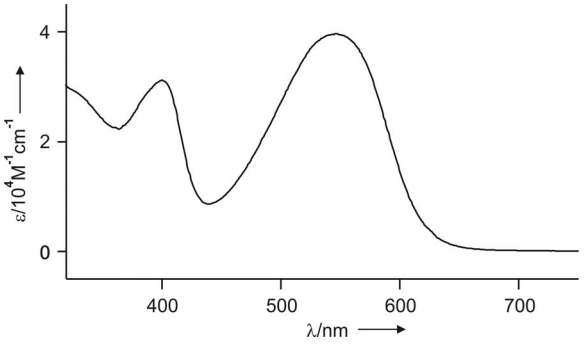

Figure 1. Absorption spectrum of **7** (dichloromethane, 298 K).

The presence of carbonyl groups in the structure of **7** was confirmed by IR spectroscopy by the very intense absorption band at 1668 cm^{-1}, attributed to the C=O stretching oscillation. Additionally, the presence of two oxygen atoms in molecules **7** and **8** was confirmed by high-resolution mass spectrometry.

^{1}H NMR Spectroscopic Analysis of 7 and 8

The ^{1}H NMR spectra of **7** and **8** are shown in Figure 2. Site-specific deuteration and several 2D experiments (COSY, NOESY, HMQC, HMBC) were used to establish the structures of all four diastereomers in solution. The crucial resonances were detected in the regions typical for conjugated, non-aromatic, acyclic systems. The ^{1}H NMR spectra reflect symmetry lowering in comparison to parent dithiaethyneporphyrin **1**. Each of the chromatographically separated benzoylbiliverdin-like species **7** and **8** give two sets of resonances in their ^{1}H NMR spectrum (Figure 2), which indicates the existence of two stereoisomers in solution. The very small excess of one stereoisomer was detected for each couple in equilibrium **7** and **8** (intensity ratio 1:1.15 and 1:1.05, respectively, at 298 K). The individual sets of signals were not assigned to specific {4*Z*,10*E*} and {4*Z*,10*Z*} of **7** and to {4*E*,10*E*} and {4*E*,10*Z*} of **8** because of a lack of unique constraints allowing their unambiguous spectroscopic distinction.

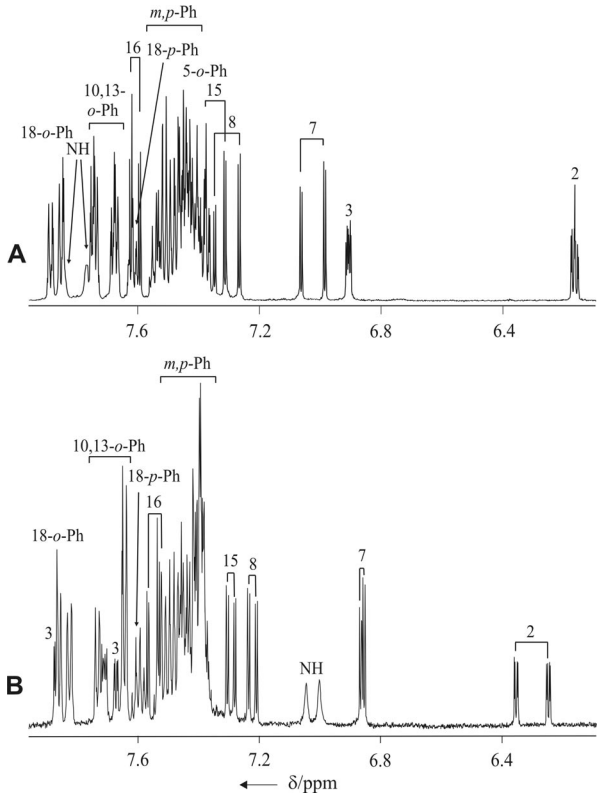

Figure 2. ^{1}H NMR ([D_2]dichloromethane, 298 K) spectra of separable couples of diastereomers **7** (A) and **8** (B). Peak labels correspond to systematic position numbering (Scheme 4) or denote proton groups: *o*-, *m*-, *p*- = *ortho*, *meta*, *para* positions of the *meso*-phenyls.

All four identified stereoisomers of the open-chain species are presented in Scheme 4. Diastereomers **7** and **8** differ by the fixed orientation of the terminal pyrrolone unit and were separated chromatographically. The NH group in **7** is oriented *trans* with respect to the 5-phenyl substituent, whereas the same fragment in **8** has a *cis* orientation. Additionally, each of these species exists as an *E* and *Z* diastereomer depending on the geometry around the flexible cumulene fragment.

The separation of the {4*Z*,10*E*} and {4*Z*,10*Z*} diastereomers of **7** identified in the ^{1}H NMR spectrum of the mixture was unsuccessful with the application of column chromatography on silica gel or basic alumina. Nevertheless, the use of HPLC (column with chiral bed; hexane/2-propanol, 4:1) allowed two fractions to be separated, which were immediately placed in a fridge icebox (–18 °C) to restrict the interconversion of diastereomers. Each of the two fractions was again injected immediately on the column without evaporation of the solvent. It was found that in both cases, besides the main peak, a second fraction, initially of small intensity, was detected. When each of the two fractions was injected on the column after storage for 30 min at room temperature, two peaks of about compar-

able intensity were always observed. The HPLC experiments clearly demonstrated that separation of the diastereomers of **7** is possible, however, both fractions equilibrate over 10 min at 298 K. The process is noticeably slower in the –18 to +4 °C temperature range and requires up to 2 h.

Similarly to **7** or **8**, in the case of cumulenes containing two pairs of ferrocenyl/phenyl termini a 1:1 mixture of *Z* and *E* diastereomers, inseparable by chromatographic methods, was also obtained.[26] However, the *Z* and *E* isomers of several fluorinated butatrienes were readily isolated by chromatography.[27] For a number of separated *E* and *Z* fluorinated butatrienes, thermal isomerization was examined in triglyme solvent.[27b] The thermodynamic equilibrium was achieved after 6 h at 110 °C.

Unique dipolar couplings between the NH proton of the pyrrolone unit and the H7 proton of the thiophene ring observed in the NOESY map for both diastereomers of **7** (Figure 3A) were essential to assign all resonances in the ^{1}H NMR spectrum. The crucial role for the complete assignment of **8** (Figure 3B) was given to the dipolar coupling observed for the NH proton and the 5-*ortho*-phenyl protons, as well as the one experienced between H3 and H7. The contact between H15 and 13-*o*-Ph in all diastereomers observed in solution confirms the conserved arrangement of the benzoylthienyl substituent as presented in Scheme 4.

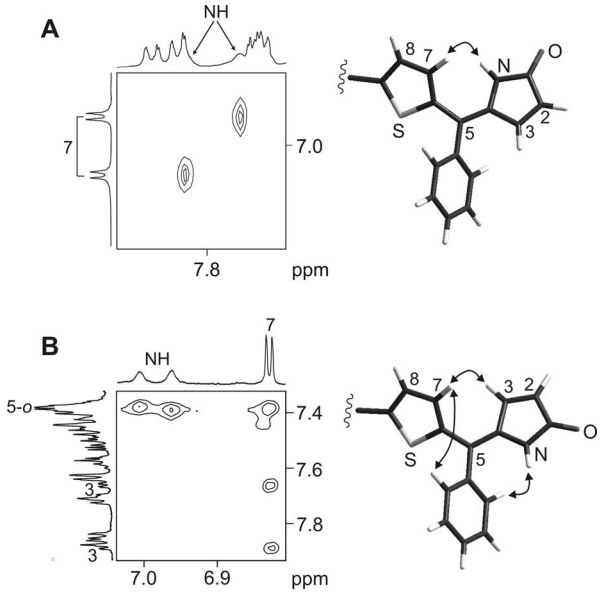

Figure 3. Fragment of the NOESY map ([D_2]dichloromethane, 298 K) for **7** (A) and **8** (B) with crucial NOE contacts.

For each diastereomer of **7** and **8**, the ^{1}H NMR spectrum displays three AB systems attributed to the β protons of two thiophene units and one pyrrolone fragment (Figure 2). The detected four-bond scalar couplings between NH and the β-pyrrole protons H2 and H3 ($^4J_{H,H}$ = 1.2–1.8 Hz) enable the pyrrolone resonances to be identified.

In the case of **7**, the H2 and H3 β-pyrrolic peaks exist as multiplets at δ = 6.91 and 6.16 ppm (Figure 2A). In contrast to **7**, the β-pyrrolic protons for each stereoisomer of **8** give nicely resolved AB systems (δ = 7.66, 6.28 ppm and 7.89, 6.42 ppm; Figure 2B). The *ortho*-phenyl protons give well-defined peaks, and their identification was possible by analysis of the NOESY map, whereas the remaining *meta*- and *para*-phenyl protons resonate in the strongly crowded 7–8 ppm region, which makes them difficult to assign.

The presence of two different carbonyl groups in each stereoisomer was confirmed by ^{13}C NMR spectroscopy. In the spectrum of **7**, signals at δ = 187.6 and 187.7 ppm were assigned to the benzoyl groups of both stereoisomers **7A** and **7B**, and one resonance from the carbonyl group of the pyrrole fragments was detected at δ = 171.9 due to coincidental overlapping. However, the **8A** and **8B** isomers give four peaks at δ = 187.5, 187.7 ppm and δ = 170.8, 171.0 ppm attributed to the benzoyl and pyrrolone units, respectively.

The exchange cross-peaks detected in the ROESY map link two resonances assigned to the equivalent hydrogen atoms in {4*Z*,10*E*} and {4*Z*,10*Z*} of **7** or {4*E*,10*E*} and {4*E*,10*Z*} of **8** (Figure 4A,B) at 350 K in [D_8]toluene. The observed correlations can be attributed to thermal *E*–*Z* isomerization reflecting a rotation around the cumulene moiety.

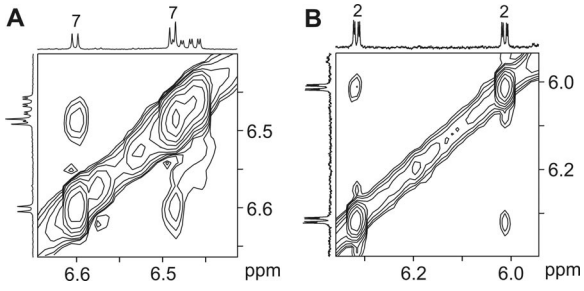

Figure 4. Fragments of the ROESY ([D_8]toluene, 350 K) spectra of **7** (A) and **8** (B) showing exchange cross-peaks between two signals of the same proton of different stereoisomers **7**: {4*Z*,10*E*} and {4*Z*,10*Z*}; **8**: {4*E*,10*E*} and {4*E*,10*Z*}. The exchange cross-peaks are positive with respect to the diagonal.

X-ray Analysis

The molecular structures of open-chain isomers {4*Z*,10*E*} **7A** and {4*E*,10*E*} **8A′** were determined by X-ray diffraction studies, and graphic representations are shown in Figure 5. The crystal structure is consistent with the spectroscopic observations for diastereomer **7A**. In contrast, two different rotamers **8A** and **8A′** with respect to the single C13–C14 and C5–C6 bonds were observed in solution and in the solid state, respectively (see also Figure 6). The bond length patterns in the C_{sp^2}–C_{sp}–C_{sp}–C_{sp^2} (C10–C11–C12–C13) unit of **7A** and **8A′** reflect the cumulene structure.[27a,28]

The structures of **7A** and **8A′** differ essentially by the geometry around double C4–C5 bond giving *E* and *Z* arrangements, respectively. In structure **7A**, the NH group is oriented *trans* to the 5-aryl, whereas in isomer **8A′** the same group displays a *cis* orientation. Additionally, the arrangement of the pyrrolone residue and the phenyl group around C5–C6 is different for each isomer. Otherwise, both struc-

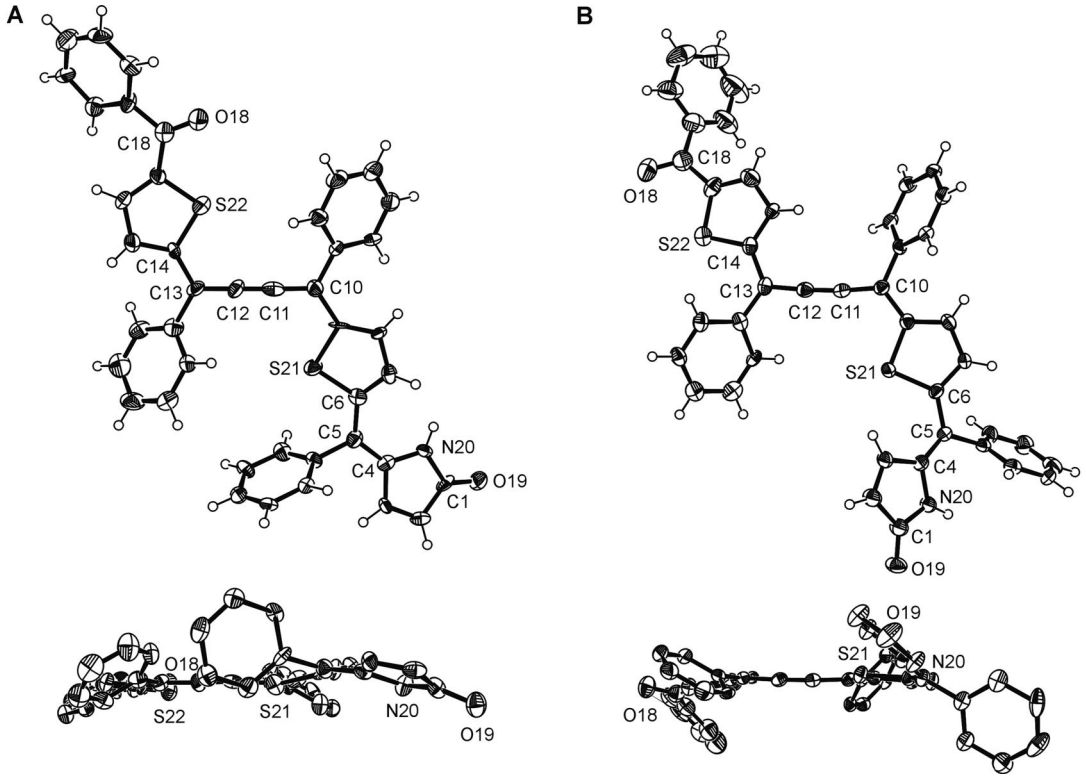

Figure 5. Molecular structures of **7A** (A) and **8A′** (B). Top: front view; bottom: side view (H atoms are omitted for clarity). The vibrational ellipsoids represent 50% probability. Selected bonds lengths: 1.37(1), 1.22(1), 1.33(1) Å and 1.358(6), 1.252(6), 1.369(6) Å in the C_{sp^2}–C_{sp}–C_{sp}–C_{sp^2} (C10–C11–C12–C13) unit of **7A** and **8A′**, respectively. For **7A**, the C1–O19 and C18–O18 bonds are 1.253(9) and 1.204(9) Å, respectively, and for **8A′** they are 1.243(5) and 1.256(6) Å, respectively.

tures vary by the conformation of the benzoylthienyl substituent around the C13–C14 bond. In **7A**, the sulfur atom and the carbonyl group of the benzoylthienyl moiety are oriented in toward the molecule, whereas in isomer **8A′**, the opposite orientation was documented.

DFT Calculations

The theoretical approach to find relative energies was involved. Initially, a simplified approach (PM3) allowed six open-chain isomers related to the structures observed in solution and in the solid state to be selected; these isomers were eventually subjected to DFT optimization at the B3LYP/6-31G** level of theory. The final geometries are shown in Figure 6. In each case a genuine energy minimum was obtained. The very small energy difference observed between suitable diastereomers accounts for their coexistence in solution (0.48 kcal/mol for **7A**/**7B**, 0.63 kcal/mol for **8A**/**8B**, and 1.24 kcal/mol for **8A′**/**8B′**; Supporting Information, Table S1).

The bond lengths are preserved in all isomers and are similar to that observed in the corresponding crystal structures (Supporting Information, Table S7). In fact they are altered in accord with the valence bond structures shown in Scheme 4. The C10–C11, C11–C12, and C12–C13 bonds orders of **7A**, **7B**, **8A**, **8A′**, **8B**, and **8B′** were estimated by using Wiberg bond indices (Supporting Information, Table S2).[29,30] The appropriate values approach 1.5, 2.2, and 1.5, respectively, reflecting the noticeable cumulene character of the C10–C11–C12–C13 fragment.

^{1}H NMR chemical shifts calculated for **7A**, **7B**, **8A**, and **8B** by using the GIAO B3LYP/6-31G** method are given in the Supporting Information (Tables S3 and S4). The electronic spectra were simulated by time-dependent DFT by using the B3LYP functional and DFT-optimized geometries. The appropriate diagrams are presented in the Supporting Information (Figures S3–S6). The theoretical results qualitatively correlate with the experimental data for both NMR and electronic spectroscopy. A more detailed analysis is not reasonable, as the spectroscopic data reveal a sum of spectroscopic response of two species remaining in thermodynamic equilibrium.

Conclusions

The reported results present dithiaethyneporphyrin, an aromatic contracted porphyrinoid, as a reactive compound when exposed to oxygen in the presence of light. The peculiar, regioselective photooxidation at the C_α–C_{meso} bond adjacent to the pyrrole ring cleanly provides a novel open-chain triheterocyclic derivative, for which four stereoisomers were detected. Diastereomers {4*Z*,10*E*}, {4*Z*,10*Z*}, {4*E*,10*E*}, and {4*E*,10*Z*} (the arrangement with respect to the C4–C5 and C10···C13 conjugated bonds given) differ by

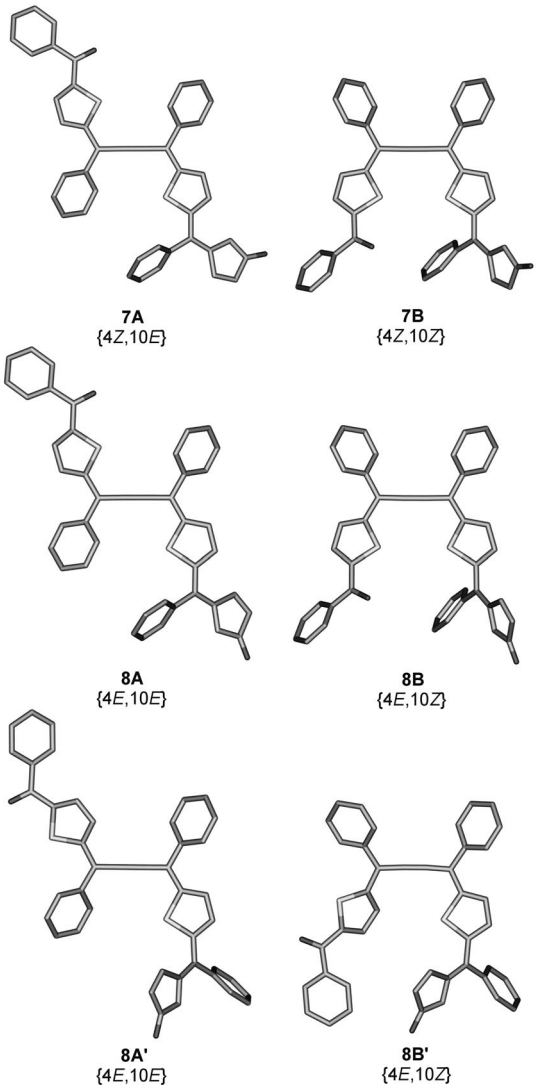

Figure 6. Geometries of the diastereomers of **7** and **8** obtained by DFT optimization at the level B3LYP/6-31G**.

the orientation of the terminal pyrrolone unit with respect to the 5-phenyl substituent and by the geometry around the cumulene fragment. Their thermal isomerization, {4*Z*,10*E*}–{4*Z*,10*Z*} and {4*E*,10*E*}–{4*E*,10*Z*}, was observed. In view of the reported findings it remains to be explored if an emerging group of three-dentate porphyrinoids including subporphyrin, subpyriporphyrins, and vacataporphyrin will undergo analogous photooxidation cleavage.

Experimental Section

Solvents and Reagents: [D_2]Dichloromethane and [D_8]toluene (CIL) were used as received. [D]Chloroform (CIL) was passed through basic Al_2O_3 before use. 3,8,13,18-Tetraphenyl-19,21-dithiaethyneporphyrin and its deuterated analogues were all obtained according to a previously described procedure.[1a]

Instrumentation: NMR spectra were recorded with high-field spectrometers (^{1}H: 500 MHz, ^{13}C: 126 MHz and ^{1}H: 600 MHz, ^{13}C: 151 MHz) equipped with either a broadband inverse gradient probehead or a direct broadband probehead. Proton data are referenced to the residual solvent signals. Absorption spectra were recorded with a diode array spectrometer. High-resolution mass spectra were recorded by using the electrospray ionization technique. HPLC experiments were carried out with a Varian ProStar 210 equipped with a semipreparative Chiralpak AI 1.0 × 25.0 column. Hexane/2-propanol (4:1) was used as the eluent with a flow rate of 3 mL/min and UV/Vis detection at 220 and 254 nm.

5-({5-[4-(5-benzoylthiophen-2-yl)-1,4-diphenylbuta-1,2,3-trienyl]thiophen-2-yl}(phenyl)methylene)-1*H*-pyrrol-2(5*H*)-one (7 and 8): Exposure of **1** (10 mg, 0.015 mmol) dissolved in CH_2Cl_2 (250 mL) to atmospheric oxygen over a period of 20–30 h resulted in the conversion of orange **1** into a pink compound identified as a mixture of **7** and **8**. The products were purified by chromatography on basic alumina (grade III, CH_2Cl_2) and recrystallized from CH_2Cl_2/hexane. Data for **7**: Yield: 6.7–7.7 mg (70–80%). UV/Vis (CH_2Cl_2): λ (logε) = 401 (4.5), 547 nm (4.6). ^{1}H NMR (600 MHz, CD_2Cl_2, 298 K): δ = 7.88 (d, $^3J_{H,H}$ = 7.9 Hz, 2 H, 18-*o*-Ph); 7.85 (d, $^3J_{H,H}$ = 7.9 Hz, 2 H, 18-*o*-Ph); 7.84 (s, 1 H, NH); 7.77 (s, 1 H, NH); 7.74 (m, 4 H, 10,13-*o*-Ph); 7.68 (m, 4 H, 10,13-*o*-Ph); 7.65–7.36 (m, 28 H, *m*-,*p*-Ph, 5-*o*-Ph); 7.62, 7.38 (AB, $^3J_{H,H}$ = 4.1 Hz, 2 H, 15,16-H); 7.59, 7.31 (AB, $^3J_{H,H}$ = 4.1 Hz, 2 H, 15,16-H); 7.35, 7.06 (AB, $^3J_{H,H}$ = 4.1 Hz, 2 H, 7,8-H); 7.27, 6.99 (AB, $^3J_{H,H}$ = 4.1 Hz, 2 H, 7,8-H); 6.91 (m, 2 H, 2,3-H), 6.16 (m, 2 H, 2,3-H) ppm. ^{13}C NMR (126 MHz, $CDCl_3$, 298 K): δ = 187.7, 187.6, 171.9, 151.9, 146.8, 146.6, 146.3, 146.2, 145.0, 144.1, 143.9, 143.7, 143.6, 138.3, 138.1, 137.6, 137.5, 137.3, 137.2, 137.1, 137.0, 135.8, 135.6, 135.5, 131.5, 131.4, 131.2, 130.0, 129.3, 129.2, 129.1, 129.0, 128.9, 128.8, 128.6, 128.5, 128.4, 128.3, 128.2, 126.7, 123.8, 121.0, 118.2, 118.1, 116.5, 116.3 ppm. IR (KBr): $\tilde{\nu}$ = 1668.2 cm^{-1} (C=O). HRMS (ESI): calcd. for $[C_{42}H_{27}NO_2S_2 + H]^+$ 642.1561; found 642.1560. Data for **8**: Yield: 1–2 mg (10–20%).^{1}H NMR (600 MHz, CD_2Cl_2, 298 K): δ = 7.89, 6.38 (AB, $^3J_{H,H}$ = 5.8 Hz, $^4J_{H,H}$ = 1.8 Hz, 2 H, 2,3-H); 7.88 (d, $^3J_{H,H}$ = 7.8 Hz, 2 H, 18-*o*-Ph); 7.85 (d, $^3J_{H,H}$ = 7.8 Hz, 2 H, 18-*o*-Ph); 7.76 (d, $^3J_{H,H}$ = 7.9 Hz, 2 H, 10-*o*-Ph); 7.73 (m, 2 H, 13-*o*-Ph); 7.70, 6.27 (AB, $^3J_{H,H}$ = 5.7 Hz, $^4J_{H,H}$ = 1.2 Hz, 2 H, 2,3-H); 7.67 (m, 4 H, 10,13-*o*-Ph); 7.63 (t, $^3J_{H,H}$ = 7.6 Hz, 1 H, 18-*p*-Ph), 7.62 (t, $^3J_{H,H}$ = 7.6 Hz, 1 H, 18-*p*-Ph); 7.59, 7.30 (AB, $^3J_{H,H}$ = 4.0 Hz, 2 H, 15,16-H); 7.56, 7.33 (AB, $^3J_{H,H}$ = 4.2 Hz, 2 H, 15,16-H); 7.57–7.38 (m, 26 H, 5-Ph, 10,13-*m*,*p*-Ph, 18-*m*-Ph); 7.26, 6.89 (AB, $^3J_{H,H}$ = 4.0 Hz, 2 H, 7,8-H); 7.23, 6.88 (AB, $^3J_{H,H}$ = 3.9 Hz, 2 H, 7,8-H); 7.07, 7.03 (2 s, 2 H, NH) ppm. ^{13}C NMR (151 MHz, $CDCl_3$, 298 K): δ = 187.7, 187.5, 171.0, 170.8, 152.1, 151.9, 146.5, 146.3, 146.2, 144.8, 144.6, 144.2, 144.0, 143.7, 143.5, 138.3, 138.1, 137.9, 137.6, 137.5, 137.34, 137.27, 137.22, 137.0, 135.83, 135.79, 135.73, 135.5, 135.4, 132.3, 132.2, 131.7, 131.5, 131.2, 130.0, 129.99, 129.97, 129.29, 129.24, 129.18, 129.09, 129.06, 129.0, 128.9, 128.84, 128.76, 128.72, 128.68, 128.54, 128.5, 128.4, 128.3, 128.1, 128.0, 125.7, 125.2, 121.7, 121.5, 118.53, 118.48, 115.9, 115.7 ppm. HRMS (ESI): calcd. for $[C_{42}H_{27}NO_2S_2 + Na]^+$ 664.1375; found 664.1337.

Structure Analysis: X-ray crystal structure data for **7A** (100 K) was obtained from crystals prepared by slow diffusion of hexane into a solution of **7** in CH_2Cl_2. Dark purple crystals, $C_{42}H_{27}NO_2S_2$, size 0.12 × 0.08 × 0.03 mm^3, triclinic, space group $P\bar{1}$, a = 8.745(2) Å, b = 13.073(2) Å, c = 15.305(4) Å, α = 65.05(2)°, β = 79.00(2)°, γ = 79.05(2)°, V = 1545.5(6) Å^3, λ = 0.71073 Å, $\rho_{calcd.}$ = 1.379 g cm^{-3}, Z = 2. Total number of reflection collected: 13493, number of independent reflections: 6093, of which 6093 were included in the refinement of 428 parameters, μ = 0.213 mm^{-1}. Structure was solved

by using direct methods with SHELXS-97 and refined against $|F|^2$ using SHELXL-97 (G. M. Sheldrick, University of Gottingen, Germany, 1997), final $R1/wR2$ indices [for $I > 2\sigma(I)$]: 0.0863/0.1190; max/min residual electron density: +0.304/–0.287 e Å^{-3}. H atoms were fixed in idealized positions by using the riding model constraints. X-ray crystal structure data for **8A′** (293 K) was obtained from crystals prepared by slow diffusion of heptane into a solution of **8** in CH_2Cl_2. Dark purple crystals, $C_{42}H_{27}NO_2S_2{\cdot}CH_2Cl_2$, size $0.1 \times 0.08 \times 0.04$ mm^3, triclinic, space group $P\bar{1}$, a = 9.889(1) Å, b = 10.522(1) Å, c = 17.617(2) Å, α = 85.04(1)°, β = 78.31(1)°, γ = 76.48(1)°, V = 1744.1(3) Å^3, λ = 0.71073 Å, $\rho_{calcd.}$ = 1.384 g cm^{-3}, Z = 2. Total number of reflection collected: 19465, number of independent reflections: 9903, of which 9903 were included in the refinement of 454 parameters, μ = 0.346 mm^{-1}. Structure was solved by using direct methods with SHELXS-97 and refined against $|F|^2$ by using SHELXL-97 (G. M. Sheldrick, University of Gottingen, Germany, 1997), final $R1/wR2$ indices [for $I > 2\sigma(I)$]: 0.0787/0.1812; max/min residual electron density: +0.600/–0.501 e Å^{-3}. The disordered molecule of dichloromethane is present. H atoms were fixed in idealized positions by using the riding model constraints.

CCDC-779017 (for **7A**) and -779018 (for **8A′**) contain the supplementary crystallographic data for this paper. These data can be obtained free of charge from The Cambridge Crystallographic Data Centre via www.ccdc.cam.ac.uk/data_request/cif.

Computational Chemistry: DFT calculations were performed by using Gaussian 03.[31] Geometry optimizations were carried out within unconstrained C_1 symmetry, with starting coordinates pre-optimized using semiempirical methods. Becke's three parameter exchange functional[32] with the gradient-corrected correlation formula of Lee, Yang, and Parr (B3LYP)[33] was used with the 6-31G** basis set. The structures were found to have converged to a minimum on the potential energy surface; the resulting zero-point vibrational energies were included in the calculation of relative energies. The Wiberg[29] bond indicates were obtained from NBO[30] calculation. Absolute ^{1}H shielding values were calculated at the GIAO-B3LYP/6-31G** level of theory by using B3LYP/6-31G** geometries. The chemical shift values were subsequently calculated relative to tetramethylsilane (TMS, absolute shielding: 31.75 ppm). The electronic spectra were simulated by time-dependent DFT by using the B3LYP functional and B3LYP geometries.

Supporting Information (see footnote on the first page of this article): Relative energies for all stereoisomers, calculated electronic spectra and ^{1}H NMR shifts, calculated and measured (X-ray) bonds for **7A** and **8A′**, calculated Cartesian coordinates.

Acknowledgments

The work was supported by the Ministry of Science and Higher Education (Grant N N204 013536). Quantum chemical calculations were carried out at the Supercomputer Centers of Poznań.

[1] a) A. Berlicka, L. Latos-Grażyński, T. Lis, *Angew. Chem. Int. Ed.* **2005**, *44*, 5288–5291; b) A. Berlicka, N. Sprutta, L. Latos-Grażyński, *Chem. Commun.* **2006**, 3346–3348.

[2] M. Pawlicki, L. Latos-Grażyński, "Carbaporphyrins – Synthesis and Coordination Properties" in *Handbook of Porphyrin Science with Applications to Chemistry, Physics, Materials Science Engineering, Biology and Medicine* (Eds.: K. M. Kadish, K. M. Smith, R. Guilard), World Scientific Publishing, Singapore, **2010**, pp. 104–192.

[3] A. Berlicka, L. Latos-Grażyński, *Inorg. Chem.* **2009**, *48*, 7922–7930.

[4] L. Flamigni, D. T. Gryko, *Chem. Soc. Rev.* **2009**, *38*, 1635–1646.

[5] R. Myśliborski, L. Latos-Grażyński, L. Szterenberg, T. Lis, *Angew. Chem. Int. Ed.* **2006**, *45*, 3670–3674.

[6] Y. Inokuma, J. H. Kwon, T. K. Ahn, M.-C. Yoo, D. Kim, A. Osuka, *Angew. Chem. Int. Ed.* **2006**, *45*, 961–964.

[7] M. S. Rodríguez-Morgade, S. Esperanza, T. Torres, J. Barberá, *Chem. Eur. J.* **2005**, *11*, 354–360.

[8] a) N. Kobayashi, Y. Takeuchi, A. Matsuda, *Angew. Chem. Int. Ed.* **2007**, *46*, 758–760; b) Y. Inokuma, Z. S. Yoon, D. Kim, A. Osuka, *J. Am. Chem. Soc.* **2007**, *129*, 4747–4761; c) Y. Takeuchi, A. Matsuda, N. Kobayashi, *J. Am. Chem. Soc.* **2007**, *129*, 8271–8281; d) E. Tsurumaki, Y. Inokuma, S. Easwaramoorthi, J. M. Lim, D. Kim, A. Osuka, *Chem. Eur. J.* **2009**, *15*, 237–247; e) E. A. Makarova, S. Shimizu, A. Matsuda, E. A. Luk′yanets, N. Kobayashi, *Chem. Commun.* **2008**, 2109–2111; f) Y. Inokuma, S. Easwaramoorthi, S. Y. Jang, K. S. Kim, D. Kim, A. Osuka, *Angew. Chem. Int. Ed.* **2008**, *47*, 4840–4843; g) Y. Inokuma, S. Easwaramoorthi, S. Y. Jang, K. S. Kim, D. Kim, A. Osuka, *Angew. Chem. Int. Ed.* **2008**, *47*, 4840–4843; h) Y. Inokuma, A. Osuka, *Chem. Eur. J.* **2009**, *15*, 6863–6876; i) S. Easwaramoorthi, J.-Y. Shin, S. Cho, P. Kim, Y. Inokuma, E. Tsurumaki, A. Osuka, D. *Kim*, *Chem. Eur. J.* **2009**, *15*, 12005–12017; j) S. Saito, K. S. Kim, Z. S. Yoon, D. Kim, A. Osuka, *Angew. Chem. Int. Ed.* **2007**, *46*, 5591–5593; k) S. Hayashi, Y. Inokuma, S. Easwaramoorthi, K. S. Kim, D. Kim, A. Osuka, *Angew. Chem. Int. Ed.* **2010**, *49*, 321–324.

[9] A. Młodzianowska, L. Latos-Grażyński, L. Szterenberg, M. Stępień, *Inorg. Chem.* **2007**, *46*, 6950–6957.

[10] J. Skonieczny, L. Latos-Grażyński, L. Szterenberg, *Chem. Eur. J.* **2008**, *14*, 4861–4874.

[11] A. Młodzianowska, L. Latos-Grażyński, L. Szterenberg, *Inorg. Chem.* **2008**, *47*, 6364–6374.

[12] E. Pacholska-Dudziak, F. Ulatowski, Z. Ciunik, L. Latos-Grażyński, *Chem. Eur. J.* **2009**, *15*, 10924–10929.

[13] P. Ortiz de Montellano, K. Auclair in *The Porphyrin Handbook* (Eds.: K. M. Kadish, K. M. Smith, R. Guilard), Academic Press, San Diego, **2003**, vol. 12, ch. 75, pp. 183–210.

[14] B. Kräutler in *The Porphyrin Handbook* (Eds.: K. M. Kadish, K. M. Smith, R. Guilard), Academic Press, San Diego, **2003**, vol. 12, ch. 82, pp. 183–209.

[15] R. Bonnett, M. J. Dimsdale, *J. Chem. Soc. Perkin Trans. 1* **1972**, 2540–2548.

[16] B. Evans, K. M. Smith, J. A. S. Cavaleiro, *J. Chem. Soc. Perkin Trans. 1* **1978**, 768–773.

[17] a) A. L. Balch, L. Latos-Grażyński, B. C. Noll, M. M. Olmstead, N. Safari, *J. Am. Chem. Soc.* **1993**, *115*, 9053–9061; b) L. Latos-Grażyński, J. Wojaczyński, R. Koerner, J. J. Johnson, A. L. Balch, *Inorg. Chem.* **2001**, *40*, 4971–4977; c) N. Asano, S. Uemura, T. Kinugawa, H. Akasaka, T. Mizutani, *J. Org. Chem.* **2007**, *72*, 5320–5326.

[18] R. Bonnett, G. Martínez, *Tetrahedron* **2001**, *57*, 9513–9547.

[19] a) J.-H. Fuhrhop, D. Mauzerall, *Photochem. Photobiol.* **1971**, *13*, 453–458; b) G. Struckmeier, I. Thewalt, J.-H. Fuhrhop, *J. Am. Chem. Soc.* **1976**, *98*, 278–279; c) R. Bonnett, A. F. McDonagh, *J. Chem. Soc. C* **1970**, 237–238.

[20] a) K. M. Smith, S. B. Brown, R. F. Troxler, J.-J. Lai, *Photochem. Photobiol.* **1982**, *36*, 147–152; b) J. A. S. Cavaleiro, M. G. P. S. Neves, M. J. E. Hewlins, A. H. Jackson, *J. Chem. Soc. Perkin Trans. 1* **1990**, 1937–1943.

[21] H. Furuta, A. Maeda, A. Osuka, *Org. Lett.* **2002**, *4*, 181–184.

[22] M. Pawlicki, I. Kańska, L. Latos-Grażyński, *Inorg. Chem.* **2007**, *46*, 6575–6584.

[23] J. Wojaczyński, L. Latos-Grażyński, *Chem. Eur. J.* **2010**, *16*, 2679–2682.

[24] a) C. Tardieux, C. P. Gros, R. Guilard, *J. Heterocycl. Chem.* **1998**, *35*, 965–970; b) R. Paolesse, A. Froiio, S. Nardis, M. Mastroianni, M. Russo, D. J. Nurco, K. M. Smith, *J. Porphyrins Phthalocyanines* **2003**, *7*, 585–592.

[25] F. Mandoj, S. Nardis, G. Pomarico, M. Stefanelli, L. Schiaffino, G. Ercolani, L. Prodi, D. Genovese, N. Zaccheroni, F. R. Fronczek, K. M. Smith, X. Xiao, J. Shen, K. M. Kadish, R. Paolesse, *Inorg. Chem.* **2009**, *48*, 10346–10357.
[26] W. Skibar, H. Kopacka, K. Wurst, C. Salzmann, K.-H. Ongania, F. Fabrizi de Biani, P. Zanello, B. Bildstein, *Organometallics* **2004**, *23*, 1024–1041.
[27] a) P. A. Morken, N. C. Baenziger, D. J. Burton, P. C. Bachand, C. R. Davis, S. D. Pedersen, S. W. Hansen, *J. Chem. Soc., Chem. Commun.* **1991**, 566–567; b) P. A. Morken, P. C. Bachand, D. L. Swenson, D. J. Burton, *J. Am. Chem. Soc.* **1993**, *115*, 5430–5439.
[28] a) Z. Berkovitch-Yellin, L. Leiserowitz, *Acta Crystallogr., Sect. B* **1977**, *33*, 3657–3664; b) H. Schmidbaur, S. Manhart, A. Schier, *Chem. Ber.* **1993**, *126*, 2389–2391.
[29] K. B. Wiberg, *Tetrahedron* **1968**, *24*, 1083–1096.
[30] E. D. M. Glendening, J. K. Badenhoop, A. E. Reed, E. Carpentier, F. Weinhold, *NBO 4*, Theoretical Chemistry Institute, University of Wisconsin Madison, **1999**.
[31] M. J. Frisch, G. W. Trucks, H. B. Schlegel, G. E. Scuseria, M. A. Robb, J. R. Cheeseman, J. A. Montgomery Jr., T. Vreven, K. N. Kudin, J. C. Burant, J. M. Millam, S. S. Iyengar, J. Tomasi, V. Barone, B. Mennucci, M. Cossi, G. Scalmani, N. Rega, G. A. Petersson, H. Nakatsuji, M. Hada, M. Ehara, K. Toyota, R. Fukuda, J. Hasegawa, M. Ishida, T. Nakajima, Y. Honda, O. Kitao, H. Nakai, M. Klene, X. Li, J. E. Knox, H. P. Hratchian, J. B. Cross, C. Adamo, J. Jaramillo, R. Gomperts, R. E. Stratmann, O. Yazyev, A. J. Austin, R. Cammi, C. Pomelli, J. W. Ochterski, P. Y. Ayala, K. Morokuma, G. A. Voth, P. Salvador, J. J. Dannenberg, V. G. Zakrzewski, S. Dapprich, A. D. Daniels, M. C. Strain, O. Farkas, D. K. Malick, A. D. Rabuck, K. Raghavachari, J. B. Foresman, J. V. Ortiz, Q. Cui, A. G. Baboul, S. Clifford, J. Cioslowski, B. B. Stefanov, G. Liu, A. Liashenko, P. Piskorz, I. Komaromi, R. L. Martin, D. J. Fox, T. Keith, M. A. Al-Laham, C. Y. Peng, A. Nanayakkara, M. Challacombe, P. M. W. Gill, B. Johnson, W. Chen, M. W. Wong, C. Gonzalez, J. A. Pople, *Gaussian 03*, Revision C.01, Gaussian, Inc., Pittsburgh, PA, **2004**.
[32] D. Becke, *Phys. Rev. A* **1988**, *38*, 3098–3100.
[33] C. Lee, W. Yang, R. G. Parr, *Phys. Rev. B* **1988**, *37*, 785–789.

Received: June 2, 2010
Published Online: August 27, 2010

